

## CLOSURE BEHAVIOUR OF SURFACE CRACKS

N. A. FLECK<sup>1</sup>, I. F. C. SMITH<sup>2</sup> and R. A. SMITH<sup>1</sup>

<sup>1</sup>Cambridge University Engineering Department, Trumpington Street, Cambridge CB2 1PZ, England and  
<sup>2</sup>ICOM (Steel Structures), Swiss Federal Institute of Technology, CH-1015 Lausanne, Switzerland

(Received 8 February 1983)

**Abstract**—The fatigue crack closure response was investigated for a surface crack in BS4360 50B structural steel, subjected to (1) constant amplitude loading and (2) constant amplitude loading interrupted by a single peak overload. A variety of compliance techniques was employed to determine closure behaviour. The crack mouth gauge measured the bulk, plane strain closure load, while the near tip strain gauge indicated the surface, plane stress closure response. For constant amplitude loading it was found that the surface regions of a surface crack are closed for a greater portion of the load cycle than the maximum depth point. A single peak overload caused different closure and growth rate transients at the surface of the thumbnail crack and at the maximum depth point. For growth rates above  $10^{-6}$  mm/cycle, such behaviour agrees with the response of a through crack when subjected to constant amplitude loading, and a single peak overload.

### NOMENCLATURE

$a$  = crack depth, mm  
 $c$  = half surface crack length, mm  
 $2r_{p,\sigma}$  = overload plane stress plastic zone size, mm  
 $2r_{p,\epsilon}$  = overload plane strain plastic zone size, mm  
 $K$  = stress intensity factor,  $\text{MPa}\sqrt{\text{m}}$   
 $\Delta K$  = stress intensity range,  $\text{MPa}\sqrt{\text{m}}$   
 $N$  = number of cycles

$U$  = closure parameter  $\left( = \frac{K_{\max} - K_{\text{op}}}{K_{\max} - K_{\min}} \right)$

$\sigma_y$  = yield stress, MPa.

#### Subscripts

$a$  = depth direction  
 $c$  = surface direction  
max = maximum  
mean = mean  
min = minimum  
ol = overload  
op = crack opening  
th = threshold.

### INTRODUCTION

When engineering structures are subjected to cyclic loading, they may fail by the advance of a thumbnail shaped fatigue crack through a section. Such cracks may originate at surface defects caused by welding, corrosion, poor handling or machining. The rate of growth of these cracks is often assumed to be determined by the value of the stress intensity factor range. It has been found that fatigue cracks may close under tensile loads [1], thus reducing the effective stress intensity range for crack growth.

Before we can estimate the life of a structure using fracture mechanics principles, we must have an accurate stress intensity calibration for a variety of crack shapes and plate thicknesses [2]. Crack shape development is often used to evaluate the accuracy of a stress intensity calibration [3]. Such an analysis assumes that the crack closure load does not vary along the crack front.

Much work has been conducted into the effect of a single peak overload on the growth rate of through cracks [1, 4–11]. Bernard *et al.* [4] found that the growth rate transient at the centre of the specimen differed markedly from the response at the surface. They tentatively suggested that this load interaction effect was due to residual stress/crack closure phenomena, though no closure measurements were taken.

In the current study, the closure responses at the maximum depth point and surface regions of a thumbnail crack are investigated, for the cases of constant amplitude fatigue loading and a single peak overload.

### CLOSURE INSTRUMENTATION

Both ultrasonic and compliance techniques have been employed for investigating the closure response of surface cracks [12, 13–15]. Frandsen *et al.* [13] found that the load at which a compliance gauge begins to show a non-linear output differs from the load at which the acoustic impedance of the specimen begins to decrease. We conclude that acoustic and compliance techniques indicate different crack closure loads.

Recent work has shown that compliance methods give a more accurate representation of the closure load than their electrical or acoustic counterparts [16]. In this study the following compliance techniques were employed (see Fig. 1):

- (1) Crack mouth displacement gauge.
- (2) Back face strain gauge.
- (3) A recently developed push-rod gauge, useful for monitoring crack opening behaviour just behind the crack tip, at the centre of the test-piece [17]. In order to use the gauge, two parallel holes of diameter 1.5 mm were drilled just behind the maximum penetration point of the elliptical crack (Fig. 1). One hole was drilled to a depth 1 mm below the fracture plane, the other to 1 mm above. The push-rod assembly was then fastened to the specimen. On recommencing cyclic loading of the test-piece, the relative displacement of the hole bottoms was measured with a twin cantilever displacement gauge, via the push-rods. The crack closure load was deduced by locating the point at which the load/displacement trace became non-linear, as with any compliance gauge.
- (4) A 1 × 1 mm strain gauge, placed just behind the crack tip and straddling the crack plane [18]. The near tip strain gauge indicates the surface, plane stress closure response. Closure measurements were taken at 0.05 Hz, using an offset procedure [16, 19].

### SPECIMEN DESIGN

Three specimens were made from BS 4360 50B structural steel of percentage composition by weight 0.14 C, 1.27 Mn, 0.41 Si, 0.017 P, 0.004 S, 0.073 Al remainder Fe. Mechanical properties in the roll direction were, yield stress 352 MPa, tensile strength 519 MPa and elongation to failure 36%.

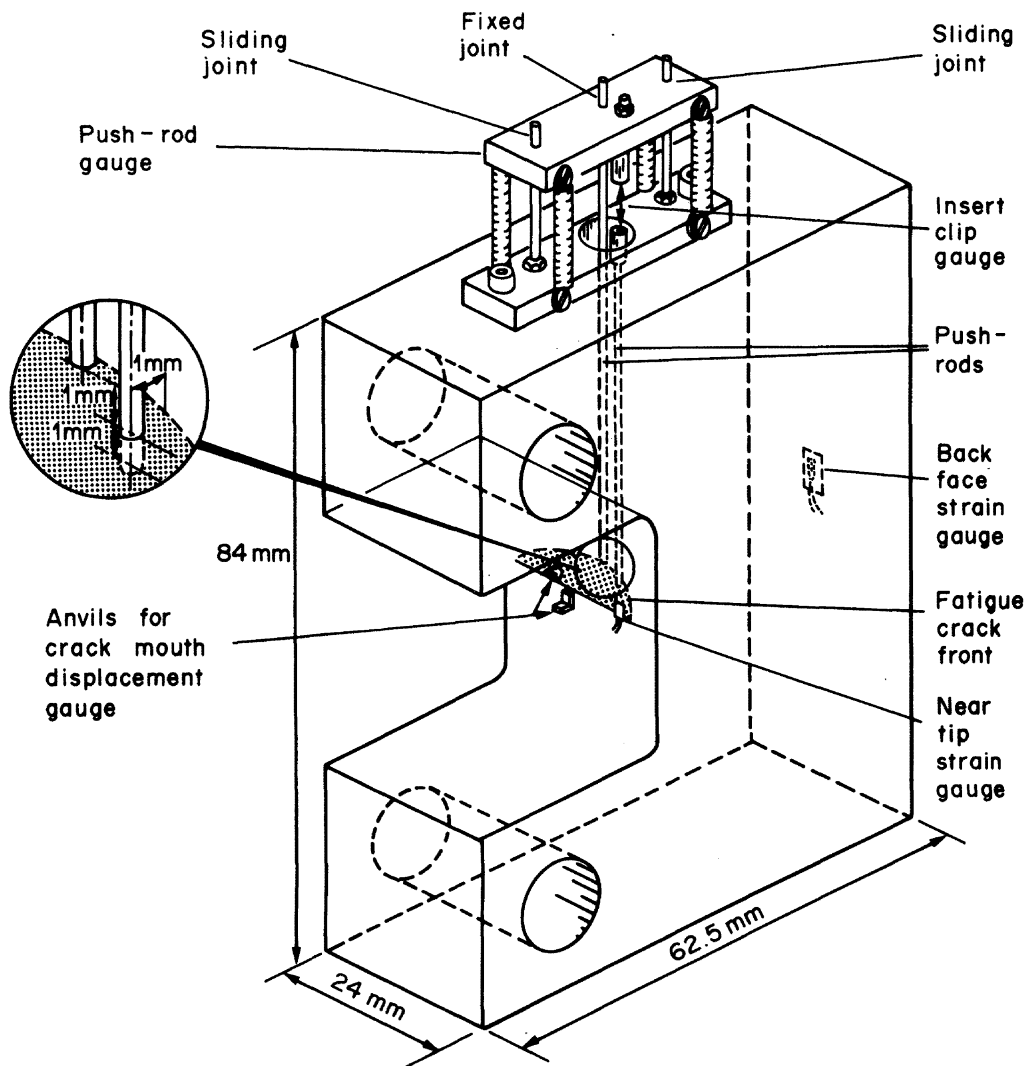


Fig. 1. Sketch of compliance gauges attached to specimen.

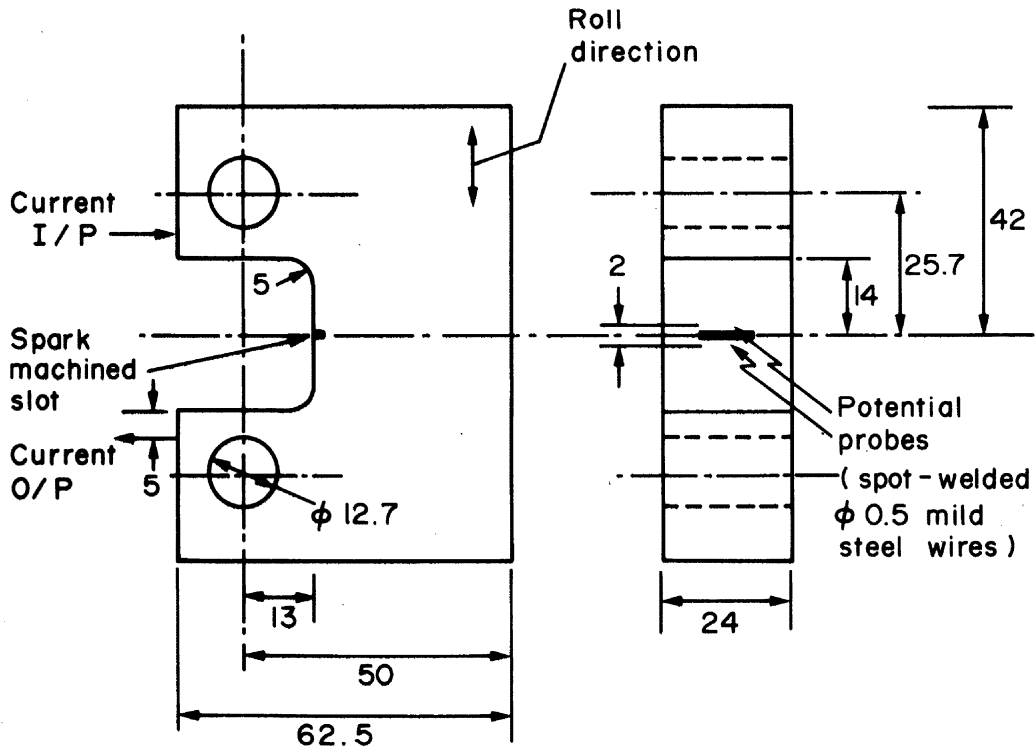
The design of the test pieces, shown in Fig. 2, was governed by the following constraints:

(1) Large values of stress intensity factor,  $K$ , were required for small loads and crack dimensions. This was achieved through the use of a bend geometry.

(2) The thickness and width of the test-piece had to be sufficient to minimise back-face and side-face effects on the  $K$  calibration, since these affect the accuracy of existing solutions [2].

(3) The test section had to be sufficiently remote from changes in section that the crack plane was free from stress concentrations. Since two slender holes needed to be drilled from the top surface of the specimen to the crack plane, to accommodate the push-rod gauge, the specimen height was limited.

(4) Access to the closure instrumentation was required at the front, back and top faces of the test-piece. Also, the front face of the test-piece had to be accessible for visual observations.



Details of spark machined slot

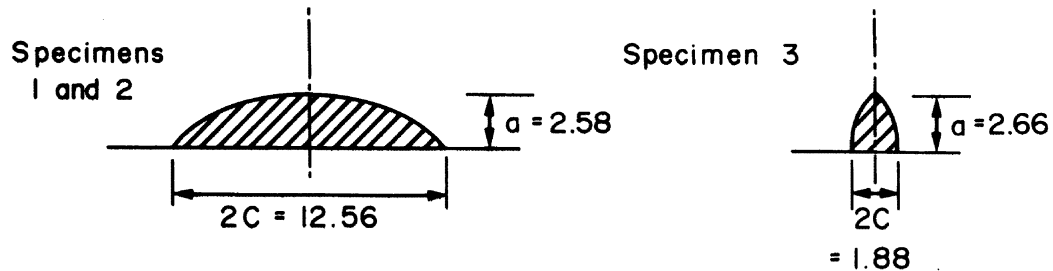


Fig. 2. Specimen geometry. Mounting positions of potential drop probe wires and current leads are shown. Dimensions are in mm.

The plane of crack growth was shown to be free of stress concentration by strain gauging an uncracked specimen. Theory and measurement both indicated that the test section was subject to a combined tensile/bending stress field with the tensile stress 20% of the bending stress at the surface of the specimen.

Slots, of geometry shown in Fig. 2, were electro-discharge machined into the test pieces, using elliptical tools of thickness 0.2 mm. The roots of the slots were sharpened, using a razor blade, to aid crack initiation. The specimens were stress relieved at 650°C for 1 h and slowly cooled in a furnace.

By employing two different shapes of slot we hoped to investigate the effect of crack shape on closure response. Unfortunately, the fatigue cracks quickly grew to similar  $a/c$  ratios, precluding a study of crack shape effects.

## CONSTANT AMPLITUDE TESTS

*Experimental*

All three specimens were employed to determine constant amplitude closure data. Fatigue cracks were grown from the initial defects at a load ratio (= minimum load/maximum load) of 0.05; loads are given in Table 1. Crack growth was monitored using both a travelling microscope and a d.c. potential drop method [20]. Briefly, a steady current of 20 A was applied to the test-piece, and the potential difference across the crack was monitored. The positions of the current leads and probe wires are given in Fig. 2.

Specimen 1 was used for calibrating the d.c. potential drop technique; the fatigue fracture surface was marked after every 0.75 mm of growth in the surface,  $c$ , direction, by applying a 10% overload to the test-piece. Closure measurements were taken immediately before and after a 10% overload, when the surface crack length,  $c$ , attained 8.3 mm. The crack opening load was determined with the crack mouth displacement, back face strain and near tip strain gauges. It was noted that the small overloads had a negligible effect on crack growth rate and closure response. At the end of the test, the test-piece was broken open and the development of crack profile observed. Thus, the relationship between potential difference across the crack and crack depth,  $a$ , was obtained.

Specimen 2 was used to gain crack growth data; no overloads were applied. When the surface crack length,  $c$ , reached 8.0 mm, the fatigue test was interrupted and closure measurements taken, using the crack mouth displacement, back face strain and near tip strain gauges. The push-rod gauge was then mounted on the test-piece and closure measurements taken with all four compliance gauges.

Specimen 3 was subjected to constant amplitude fatigue loading until the surface crack length,  $c$ , reached 4.0 mm. Crack closure measurements were taken using the crack mouth displacement, back face strain and near tip strain gauges.

Test details for the three specimens are summarised in Table 1.

*Results and discussion*

The stress intensity factor at the surface,  $\Delta K_c$ , and at the maximum depth point,  $\Delta K_a$ , were calculated from Newman and Raju's finite element results [2]. Since the ratio of crack depth to specimen width exceeded that of Newman and Raju's analysis, a finite width correction was employed [21].

The closure parameter,  $U$ , is defined by  $(K_{\max} - K_{\text{op}})/(K_{\max} - K_{\min})$ , where  $K_{\max}$ ,  $K_{\min}$  and  $K_{\text{op}}$  are the maximum, minimum and crack opening stress intensities, respectively. Closure results are given in Table 1. Both the crack mouth displacement gauge and the push-rod gauge indicated a plane strain closure value,  $U_a$ , of 0.85, for specimen 2. We may, therefore, use a crack mouth displacement gauge for monitoring the bulk, plane strain response of a thumbnail crack. The back face strain gauge was insufficiently sensitive to detect crack closure: the distance from crack tip to this gauge was much greater than the closed crack increment at minimum load.

It was noted from specimens 1–3 that the plane strain closure value,  $U_a$ , was 0.85, whilst the plane stress closure value,  $U_c$ , was 0.75; measurements were taken for  $\Delta K$  in the range 10–20 MPa $\sqrt{\text{m}}$ , and a constant crack shape,  $a/c$ , of  $0.87 \pm 0.09$ . We conclude that a greater degree of crack closure occurs at the surface than the bulk plane strain regions of the specimen.

Crack growth rates in the depth,  $a$ , direction were found to be 50% faster than growth

Table 1. Summary of test details and closure results

Specimen number	Mini- mum load (kN)	Maxi- mum load (kN)	Dimensions of spark machined slot		Initial crack dimensions for growth rate measurements		Final crack dimensions for growth rate measurements		Range in growth rates during test (mm/cycle)	Constant amplitude closure response					
			<i>a</i> (mm)	<i>c</i> (mm)	<i>a</i> (mm)	<i>c</i> (mm)	<i>a</i> (mm)	<i>c</i> (mm)		$\Delta K_c$ (MPa $\sqrt{\text{m}}$ )	$\Delta K_c$ (MPa $\sqrt{\text{m}}$ )	$U_c$ †	$U_c$ ‡		
1	1.2	24	2.58	6.28	3.02	6.54	6.84	8.74	$6 \times 10^{-6}$ - $2 \times 10^{-5}$	6.6	8.3	20.0	17.5	0.85	0.75
2	1.2	24	2.58	6.28	2.62	6.31	6.27	8.41	$4 \times 10^{-6}$ - $2 \times 10^{-5}$	6.2	8.0	19.7	17.2	0.87	0.76
3*	1.3	25	2.66	0.94	3.10	2.92	9.10	9.65	$3 \times 10^{-6}$ - $1 \times 10^{-5}$	3.8	4.0	11.8	14.2	0.83	0.73

\*Single peak overload of 48.7 kN applied when crack depth, *a*, reached 3.8 mm.

†Crack mouth displacement gauge results for specimens 1 and 3. Crack mouth displacement gauge and push-rod gauge results, for specimen 2.

‡Near tip strain gauge results.

rates in the surface,  $c$ , direction, for the same value of  $\Delta K$ . This behaviour was observed over the measured range in growth rate, i.e.  $3 \times 10^{-6}$ – $2 \times 10^{-5}$  mm/cycle. Can we explain this difference in growth rates using closure arguments?

The fatigue crack propagation response of through-cracked compact tension specimens made from BS4360 50B was recently evaluated [22]. A power-law relation between growth rate and the effective stress intensity range ( $U\Delta K$ ) was observed:

$$\frac{da}{dN} = 1.48 \times 10^{-8} (U\Delta K)^{2.86} \text{ mm/cycle} \quad (1)$$

where the growth rate,  $da/dN$ , is between  $10^{-6}$  and  $10^{-3}$  mm/cycle, and  $\Delta K$  has the units  $\text{MPa}\sqrt{\text{m}}$ . Equation (1) implies that the growth rate in the depth,  $a$ , direction should be faster than in the surface,  $c$ , direction by a factor of  $(0.85/0.75)^{2.86} = 1.43$ , for the same value of  $\Delta K$ . Since the measured growth rate was 50% faster in the depth,  $a$ , direction than the surface,  $c$ , direction, the crack closure phenomenon successfully explains the difference in growth rates.

Newman and Raju [2] successfully predicted the development of crack shape in an aluminium alloy, titanium alloy and steel by arbitrarily assuming that the stress intensity factor in the  $c$ -direction was reduced by 10%, relative to the stress intensity factor in the  $a$ -direction. This assumption is justified by the crack closure observations of the present study. It is evident that crack shape development may be used to evaluate the accuracy of a stress intensity calibration, only if the variation in closure load along the crack front is taken into account.

Tests on through-crack compact tension specimens have shown that the average plane stress closure value,  $U$ , is 0.74, and the average plane strain  $U$  value is 0.84, for  $\Delta K$  in the range 10–20  $\text{MPa}\sqrt{\text{m}}$  [22]. Since similar values were determined in the current investigation, it is deduced that the thumbnail crack shows the same closure response as an equivalent through crack.

Smith and Smith [23] have shown that the fatigue crack propagation rates of surface cracks growing from the toe of a fillet weld may be successfully predicted from long through crack data, for growth rates in the range  $10^{-6}$  to  $10^{-4}$  mm/cycle. Such behaviour is explained by the observation that the closure responses of surface and through cracks are identical, at these growth rates.

Byrne and Duggan [12] and Smith [24] found the threshold stress intensity range  $\Delta K_{\text{th}}$  of semi-elliptical cracks to be less than  $\Delta K_{\text{th}}$  for long, through cracks, at a load ratio of 0.1. Also, the surface cracks were closed for a smaller portion of the load cycle than the through cracks [12]. It is concluded from a comparison of previous work and the present study that surface cracks show a different closure response to through cracks at near threshold growth rates (below  $10^{-6}$  mm/cycles), but the same closure response at higher growth rates.

## SINGLE PEAK OVERLOAD

### *Experimental*

Specimen 3 was fatigued at a constant load range of 23.7 kN and load ratio of 0.05, except for a single 100% overload of 48.7 kN when the surface crack length,  $c$ , reached 4.00 mm. Closure response was monitored throughout the test using a crack mouth displacement, back face strain and near tip strain gauges. A new near tip strain gauge

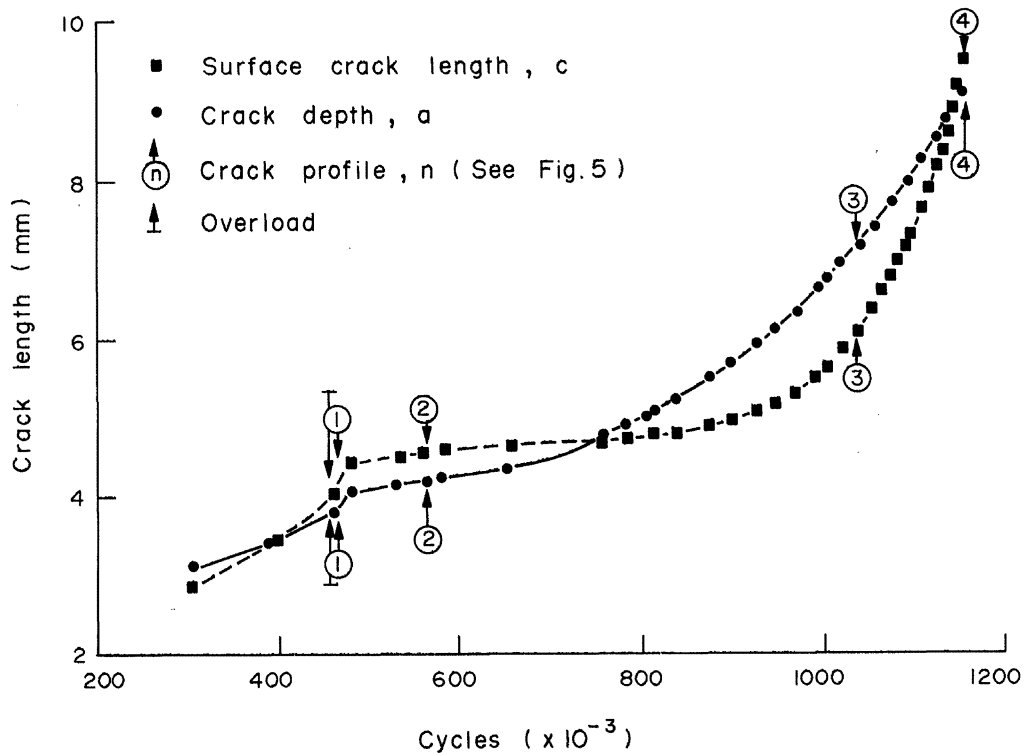


Fig. 3. Crack growth transient following a single peak overload. Specimen 3.

was applied to the test piece after every 1.5 mm of growth in the  $c$ -direction, to ensure that this gauge monitored the surface rather than bulk closure response. Since the crack shape developed in a different manner from specimens 1 and 2, due to the differences in notch shape and load history, a different potential drop calibration was required. Fortunately, changes in test frequency from 10 to 0.05 Hz marked the fatigue fracture surface, and so a new calibration curve of electrical potential difference against crack depth,  $a$ , could be produced.

To examine the way in which the fatigue crack opened after an overload, two stage acetate replicas of the crack were taken when the surface crack length,  $c$ , reached 6.1 mm. Replicas were taken at minimum, mean and maximum load of the fatigue cycle. The replication technique has been documented elsewhere [25] and has been used successfully for determining the crack opening response of through cracks subjected to constant amplitude loading [16].

#### Results and discussion

*Growth rate transient.* The effect of a single peak overload on the subsequent crack growth, crack growth rates and crack shape development is displayed in Figs 3–5. Crack growth rates were calculated using a 3 point quadratic fit. It is apparent that the crack responds to the single peak overload quite differently at the surface and at the maximum depth point.

Three stages in the evolution of crack shape were observed; the start and end of each stage was marked by a crack profile (see Fig. 5). Crack lengths and growth rates corresponding to the crack profiles 1–4 are included in Figs 3 and 4.

(1) Prior to application of the overload, the crack adjusted to a 'stable' semi-elliptical



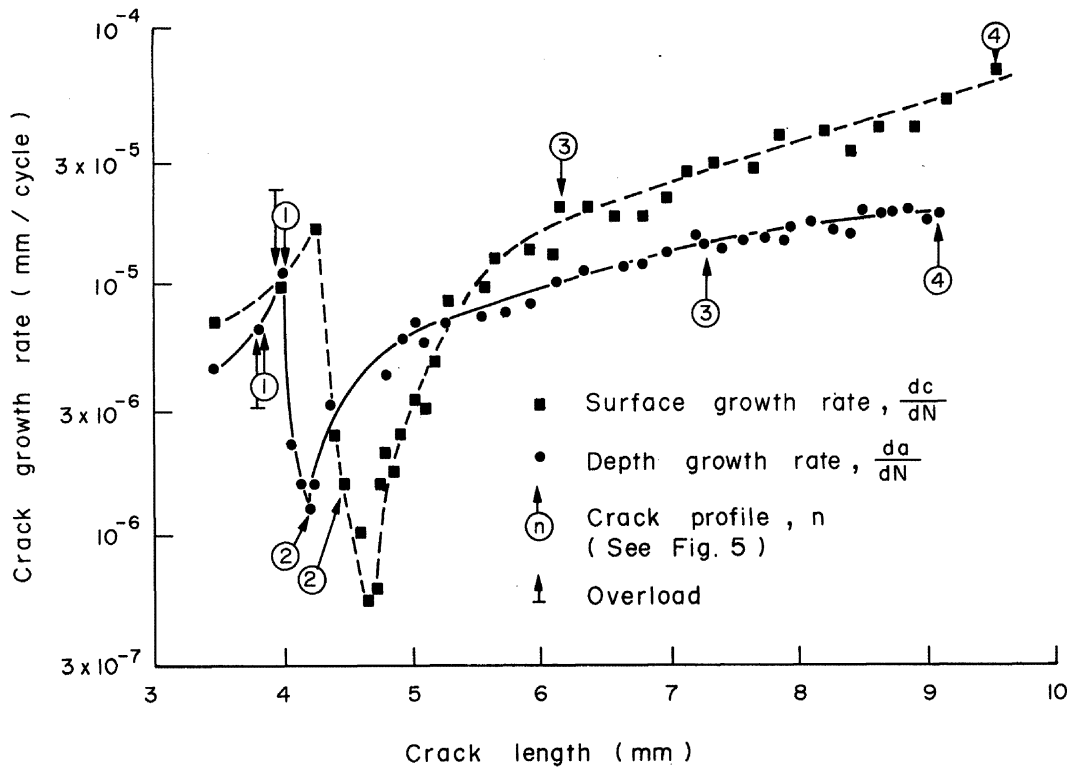


Fig. 4. Crack growth rate transient following a single peak overload. Specimen 3.

shape, profile 1. Following application of the overload, before a minimum growth rate was reached,  $c$  was retarded more than  $a$  (see Figs 3 and 4). The crack aspect ratio,  $a/c$ , dropped to below the constant amplitude value as the crack shape evolved from profile 1 to profile 2 (Fig. 5).

(2) Crack growth rates in the depth,  $a$ , direction, increased again, while growth rates in the surface,  $c$ , direction decreased to a minimum. Growth rates remained slower in the surface than depth direction and the crack aspect ratio,  $a/c$ , increased to more than the constant amplitude value. Profile 3 was adopted (see Fig. 5).

(3) Crack growth rate increased slowly in the depth,  $a$ , direction and rapidly in the surface,  $c$ , direction. The crack aspect ratio,  $a/c$ , decreased toward the curvature characteristic of constant amplitude fatigue loading, and profile 4 was assumed.

Bernard *et al.* [4] have examined the surface and bulk crack growth responses of a 75 mm thick compact tension specimen made from pressure vessel steel and subjected to a single peak overload. The growth transient at the surface of their through crack was similar to the surface growth transient of the thumbnail crack currently reported. Also, the growth transients at the centres of the through crack and thumbnail crack were the same.

The change in crack shape due to an overload influences the stress intensity calibration for the surface crack. If the constant amplitude crack shape is assumed rather than the actual crack shape (Fig. 5) errors of up to 30% for  $K$  in the  $c$ -direction, and 7% for  $K$  in the  $a$ -direction, result.

Several workers [5, 6, 10] have found good agreement between the overload affected crack growth increment of a through crack and the overload plastic zone size, defined

by:

$$2r_{p,\sigma} = \frac{1}{\pi} \left[ \frac{K_{ol}}{\sigma_y} \right]^2 \quad \text{plane stress}$$

$$2r_{p,\epsilon} = \frac{1}{3\pi} \left[ \frac{K_{ol}}{\sigma_y} \right]^2 \quad \text{plane strain}$$

where  $K_{ol}$  is the overload stress intensity and  $\sigma_y$  is the 0.2% offset yield stress.

The plane stress overload plastic zone size,  $2r_{p,\sigma}$ , is included on the plot of surface growth rate,  $dc/dN$ , against crack length (Fig. 6) while the plane strain overload plastic zone size,  $2r_{p,\epsilon}$ , is included on the plot of growth rate in the depth direction,  $da/dN$ , against crack length (Fig. 7). The overload affected crack length in the surface,  $c$ , direction is equal to  $2r_{p,\sigma}$  and the overload affected crack length in the depth,  $a$ , direction is about twice  $2r_{p,\epsilon}$ .

Previous investigators [6, 7] found that the maximum retardation in growth rate occurs after a crack growth increment of one quarter to one half the appropriate overload plastic zone size; the results of the present study are no exception, see Figs 6 and 7.

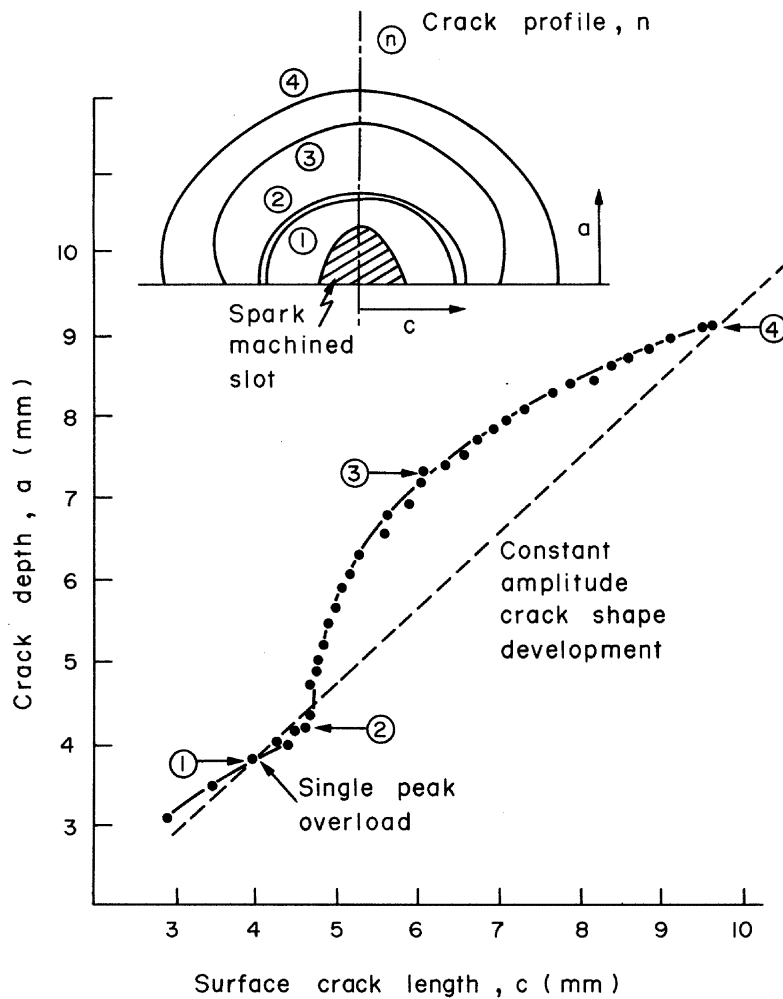


Fig. 5. Crack shape development following a single peak overload. Specimen 3.

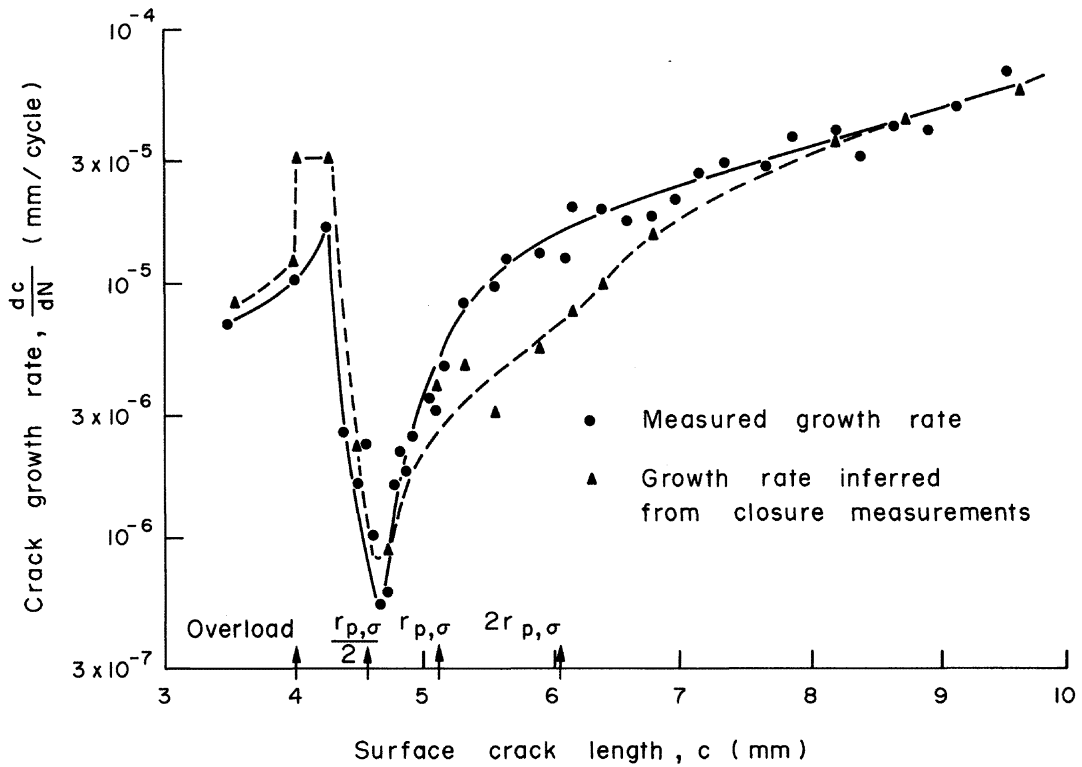


Fig. 6. Comparison of measured growth rate transient following a single peak overload with the growth rate inferred from closure measurements. Surface, plane stress response. Specimen 3.

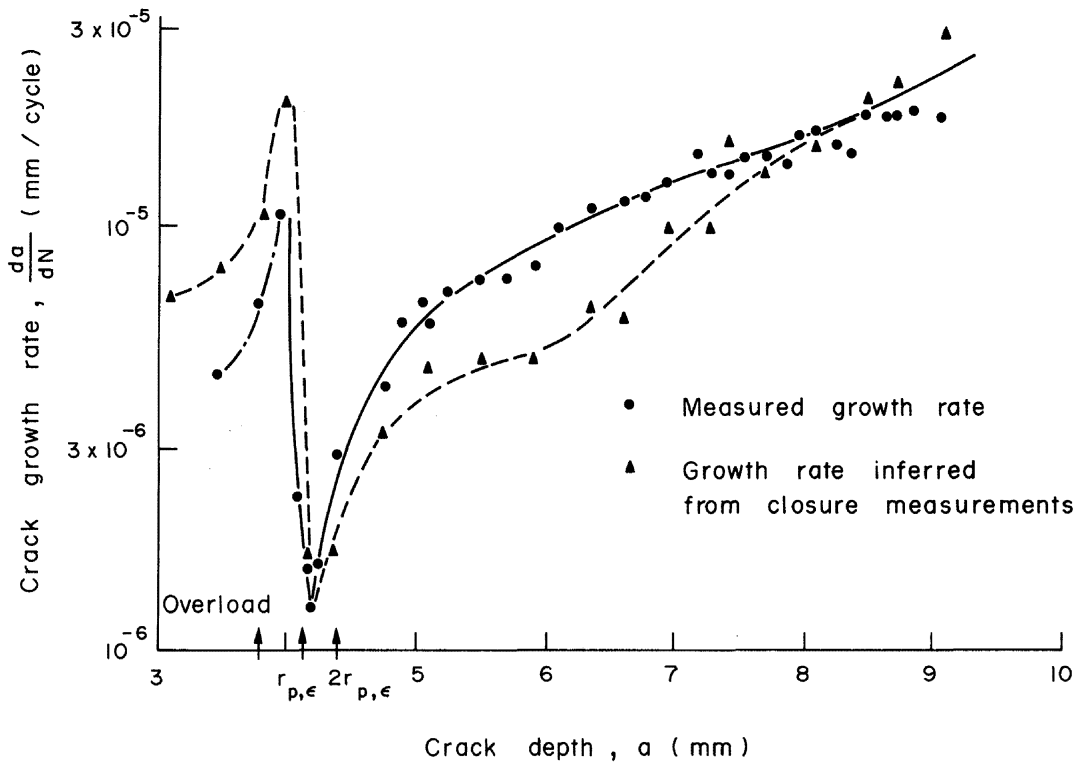


Fig. 7. Comparison of measured growth rate transient following a single peak overload with the growth rate inferred from closure measurements. Bulk, plane strain response. Specimen 3.

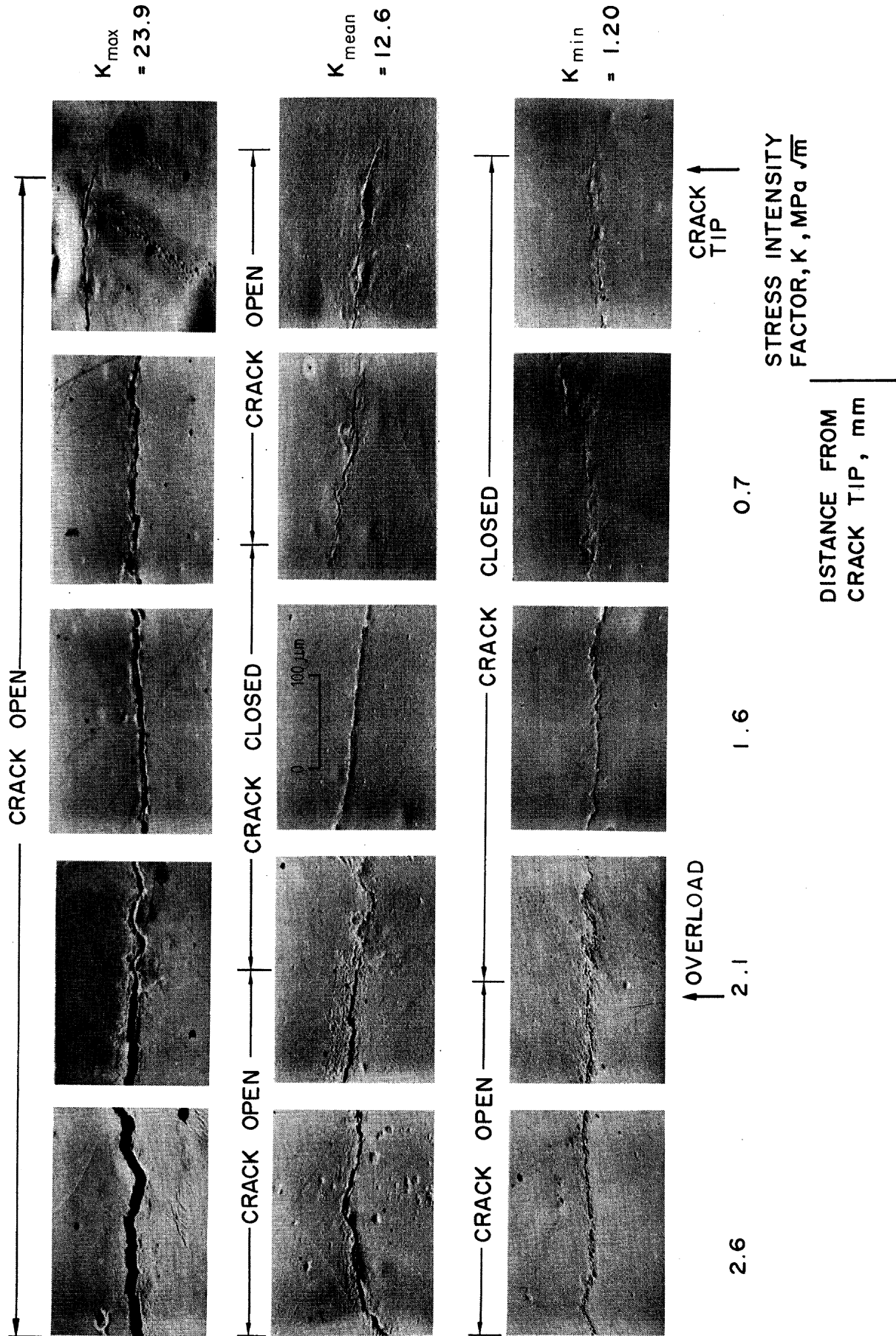


Fig. 8. Photomicrographs of double replicas, taken after a single peak overload. Discontinuous crack opening shown at mean load. Specimen 3, crack length,  $c$ , = 6.1 mm.

*Closure response.* Both the plane stress and plane strain closure values,  $U$ , decreased to a minimum after the application of the overload, and then slowly returned to the pre-overload values. In order to determine whether the closure phenomenon can successfully account for the growth rate transients, use is made of equation (1). Specifically, the surface closure transient,  $U_c$ , and stress intensity range,  $\Delta K_c$ , are substituted into equation (1) to predict the crack growth rate in the surface,  $dc/dN$ . Predicted and measured surface growth rates are compared in Fig. 6. Similarly, growth rates in the depth direction are predicted from equation (1), and compared with measured growth rates in Fig. 7.

The crack closure phenomenon appears to be the dominant cause of load interaction effects, in agreement with the findings of several investigations on through cracks [6, 8, 11].

The measured crack growth rates in the depth,  $a$ , direction before application of the overload must be regarded with suspicion as the crack is still within the influence of the starter slot. Accordingly, the crack growth rate is shown as a dash-dot curve until application of the overload in Figs 4 and 7.

It is noted from Figs 6 and 7 that after maximum retardation of growth rate, the closure load remains anomalously high and predicted growth rates are too low. Robin *et al.* [9] found the same phenomenon for through cracks in steel. Observations of crack tip replicas under the scanning electron microscope showed that the crack was open near its tip but closed further back, for part of the load range (Fig. 8). This means that the crack tip experiences cyclic displacements, for loads less than the indicated crack closure load. Measured growth rates are therefore higher than crack closure measurements would predict. This phenomenon has also been noted for through cracks in thin BS4360 50B compact tension specimens [22].

It is concluded that crack closure is able to account for the growth rate transient following a single peak overload, though compliance measurements may indicate otherwise.

## CONCLUSIONS

(1) The crack mouth gauge or push-rod gauge may be used to evaluate the plane strain closure response of a surface crack. A near tip strain gauge may be used to evaluate the surface plane stress closure response. The back face strain gauge is unable to monitor the closure load since the uncracked ligament is large in comparison with the closed crack increment at minimum load.

(2) The surface plane stress regions of an elliptical crack are closed for a larger portion of the fatigue load cycle than the maximum depth, plane strain, regions of the crack front. Such closure information is necessary for the successful prediction of crack shape development in laboratory and structural components.

(3) The closure response of a surface elliptical crack is similar to that of a through crack in a thick specimen, for growth rates in the range  $10^{-6}$ – $10^{-4}$  mm/cycle.

(4) The crack growth rates shown by a surface crack are severely retarded on application of a single peak overload. The growth rate transient at the surface of the crack is different from that at the maximum depth point of the crack. Crack closure is able to account for these load interaction effects.

(5) The responses of surface and through cracks to a single peak overload are similar.

*Acknowledgements*—The authors wish to thank the Director of British Gas Engineering Laboratories for provision of test material, and for financial aid. One of the authors (NAF) was funded by the Department of Education, Northern Ireland, another (IFCS) by the Association of Commonwealth Universities.

## REFERENCES

1. Elber W. (1971) The significance of fatigue crack closure. *Damage Tolerance in Aircraft Structures*, ASTM STP 486, pp. 230–242. American Society for Testing and Materials.
2. Newman J. C. Jr and Raju I. S. (1981) An empirical stress intensity factor equation for the surface crack. *Engng Fract. Mech.* **15**, 185–192.
3. Scott P. M. and Thorpe T. W. (1981) A critical review of crack tip stress intensity factors for semi-elliptic cracks. *Fatigue Engng Mater. Struct.* **4**, 291–309.
4. Bernard P. J., Lindley T. C. and Richards C. E. (1977) The effect of single overloads on fatigue-crack propagation in steels. *Metal Sci.* 390–398.
5. von Euw E. F. J., Hertzberg R. W. and Roberts R. (1972) Delay effects in fatigue crack propagation. Stress analysis and growth of cracks. *Proceedings of the 1971 National Symposium on Fracture Mechanics, Part I*, ASTM STP 513, pp. 230–259. American Society for Testing and Materials.
6. Mills W. J., Hertzberg R. W. and Roberts R. (1977) Load interaction effects on fatigue crack growth in A514F steel alloy. *Cyclic Stress-Strain and Plastic Deformation Aspects of Fatigue Crack Growth*, ASTM STP 637, pp. 192–208. American Society for Testing and Materials.
7. Matsuoka S. and Tanaka K. (1973) Delayed retardation phenomenon of fatigue crack growth resulting from a single application of overload. *Engng Fract. Mech.* **10**, 515–525.
8. Tanaka K., Matsuoka S., Schmidt V. and Kuna M. (1981) Influence of specimen geometry on delayed retardation phenomena of fatigue crack growth in HT80 steel and A5083 aluminium alloy. *Proceedings of the 5th International Conference on Advances in Fracture*, pp. 1789–1798. Cannes.
9. Robin C., Louah M. and Pluvillage G. (1983) Influence d'une surcharge sur la progression des fissures de fatigue dans le cas des aciers. To appear in *Mater. Elect.*
10. Wei R. P., Fenelli N. E., Unangst K. D. and Shih T. T. (1980) Fatigue crack growth response following a high load excursion in 2219–T851 aluminium alloy. *J. Engng Mater. Technol. Trans. ASME* **102**, 280–292.
11. Nowack H., Trautmann K. H., Schulte K. and Lutjering G. (1979) *Sequence Effects on Fatigue Crack Propagation; Mechanical and Microstructural Contributions*, ASTM STP 677, pp. 36–53. American Society for Testing and Materials.
12. Byrne J. and Duggan T. V. (1982) Influence of crack geometry and closure on the fatigue threshold condition. *Proceedings of the International Symposium on Fatigue Thresholds* (Edited by Bäcklund J., Blom A. F. and Beevers C. J.). EMAS Publications Ltd, Warley, U.K.
13. Fransden J. D., Inman R. V. and Buck O. (1975) A comparison of acoustic and strain gauge techniques for crack closure. *Int. J. Fract.* **11**, 345–348.
14. Buck O., Ho C. L. and Marcus H. L. (1973) Plasticity effects in fatigue crack propagation. *Engng Fract. Mech.* **12**, 23–34.
15. Buck O., Fransden J. D. and Marcus H. L. (1975) Crack tip closure and environmental crack propagation. *Engng Fract. Mech.* **7**, 167–171.
16. Fleck N. A. (1982) The use of compliance and electrical resistance techniques to characterise fatigue crack closure. Cambridge University Engineering Department Report, CUED/C/MAT/TR.89.
17. Fleck N. A. and Smith R. A. (1982) Crack closure—is it just a surface phenomenon? *Int. J. Fatigue* 157–160; Correction in *Int. J. Fatigue* 243.
18. Schmidt R. A. and Paris P. C. (1973) Threshold for fatigue crack propagation and the effects of load ratio and frequency. *Progress in Flaw Growth and Fracture Toughness Testing*, ASTM STP 536, pp. 79–94. American Society for Testing and Materials.
19. Kikukawa M., Jono M. and Tanaka K. (1976) Fatigue crack closure behaviour at low stress intensity levels. *Proc. ICM2* 254–277.
20. Smith I. F. C. and Smith R. A. (1982) Measuring fatigue cracks in fillet welded joints. *Int. J. Fatigue* **4**, 41–45.

21. Holbrook S. J. and Dover W. D. (1979) The stress intensity factor for a deep surface crack in a finite plate. *Engng Fract. Mech.* **12**, 347–364.
22. Fleck N. A. (1983) Ph.D. Thesis, Cambridge University.
23. Smith I. F. C. and Smith R. A. (1982) Fatigue crack growth in a fillet welded joint. Accepted for publication in *Engng Fract. Mech.*
24. Smith I. F. C. (1982) Advances in defect assessment for fatigue. *Metal Constr.* **14**, 605–608.
25. Brown C. W. (1980) The initiation and growth of fatigue cracks in titanium alloys. Ph.D. Thesis, Cambridge University Department of Metallurgy.